Rapid Communications

Possible superconductivity above 40 K in rhenium-doped strontium ruthenates indicated by Fourier-transform infrared spectroscopy

Yurii Aleshchenko,[1] Boris Gorshunov,[2] Elena Zhukova,[2] Andrey Muratov,[1] Alexander Dudka,[3] Rajendra Dulal,[4] Serafim Teknowijoyo,[4] Sara Chahid,[4] Vahan Nikoghosyan,[4] and Armen Gulian[4,*]

[1]*V.L. Ginzburg Center for High-Temperature Superconductivity and Quantum Materials, P.N. Lebedev Physical Institute of the Russian Academy of Sciences, 53 Leninskiy Prospekt, 119991 Moscow, Russia*

[2]*Laboratory of Terahertz Spectroscopy, Center for Photonics and 2D Materials, Moscow Institute of Physics and Technology (National Research University), 141701 Dolgoprudny, Moscow Region, Russia*

[3]*Shubnikov Institute of Crystallography of Federal Scientific Research Centre "Crystallography and Photonics" of Russian Academy of Sciences, Leninskiy Prospekt 59, 119333 Moscow, Russia*

[4]*Advanced Physics Laboratory, Institute for Quantum Studies, Chapman University, Burtonsville, Maryland 20866, USA*

(Received 30 June 2020; accepted 28 September 2020; published 27 October 2020)

Strontium ruthenates have a lot of similarities with copper oxide superconductors and are a very interesting object for investigation of mechanisms and conditions which lead to high-temperature superconductivity. We report here on multiple experimental indications of superconductivity with the onset above 40 K in strontium ruthenate doped by rhenium and selenium with chlorine used as a flux. The main experimental evidence comes from FTIR spectroscopy of this material followed by the ac and dc magnetization, as well as its heat capacity and magnetoresistance. Structural and morphological studies reveal the heterophase nature of this polycrystalline material as well as changes of lattice parameters relative to the original phases. Experimental data provide evidence of higher critical temperature on the surface compared to that in the bulk of the sample.

DOI: 10.1103/PhysRevResearch.2.042020

I. INTRODUCTION

The fascinating properties of strontium ruthenates $Sr_{n+1}Ru_nO_{3n+1}$ ($n = 1, 2, \ldots, \infty$) have garnered enormous attention [1] since the discovery of high-temperature superconductivity in cuprates. Superconductivity in ruthenates was found only for the $n = 1$ case [2] with T_c as high as 1.5 K [3]. Other representatives of this Ruddlesden-Popper family possess peculiar magnetic properties. The most pronounced magnetic order takes place at $n = \infty$: $SrRuO_3$ is a ferromagnet with Curie temperature $T_{Curie} \sim 165$ K; at $n = 2$, $Sr_3Ru_2O_7$ is an anomalous paramagnet; at $n = 3$, $Sr_4Ru_3O_{10}$ is a metamagnet [3]. The Cooper pairing in Sr_2RuO_4 was well known as a textbook example of the spin-triplet state (odd parity $S = 1$; see reviews [3–6] and references therein). Recently, NMR spectroscopy reinvestigation [7] has given compelling evidence that the superconductivity in Sr_2RuO_4 is likely to be even parity, which unequivocally demonstrates that research on the physical properties of ruthenates is far from being complete.

Another confirmation of this statement comes from the recent fascinating discovery of high-temperature superconductivity in calcium ruthenate, Ca_2RuO_4 [8]. The stoichiometric composition of this material in a single-crystalline form is a Mott insulator, while single crystals with excess oxygen are metallic above 160 K [9] and the only crystallographic difference between them lies in the c axis: 11.94 Å vs 12.35 Å. Interestingly, electrically induced insulator-metal transition has been detected via infrared nanoimaging and optical-microscopy measurements on bulk single crystal Ca_2RuO_4 [10]. Much more drastic changes occur when the thickness of Ca_2RuO_4 crystal is reduced to the nanometer range: novel quantum states including high-temperature superconductivity via resistive and magnetic measurements at 64 K have been observed [8]. This remarkable finding in micronanocrystals [11] demonstrated how rich the superconducting phenomena in ruthenates can be. It also invigorates the value of polycrystalline materials (ceramics), in which the samples in [8] were originally prepared before subsequent sonification to obtain micronanocrystals.

In this Rapid Communication, we present spectroscopic data in the FIR range obtained on polycrystalline samples of initial stoichiometric composition of $Sr_2Ru_{1-x}Re_xO_{4-y}Se_y$. The choice of this composition was made as a result of a series of experiments in which the oxygen was partially replaced by S or Se in the presence of Cl as a flux at the synthesis of $Sr_2RuO_{4-x}S(Se)_x$ and subsequent cationic substitutions for Ru (Fig. 1).

As follows from Fig. 1, temperature dependence of resistivity, ρ(T), of strontium ruthenate samples drastically changes into typical strange-metal behavior [12] at application of Cl flux and vacuum during synthesis (details can be found in [13]). Moreover, inclination towards zero resistivity at $T \to 0$ K appears at further substitution of chalcogens

*Corresponding author: gulian@chapman.edu

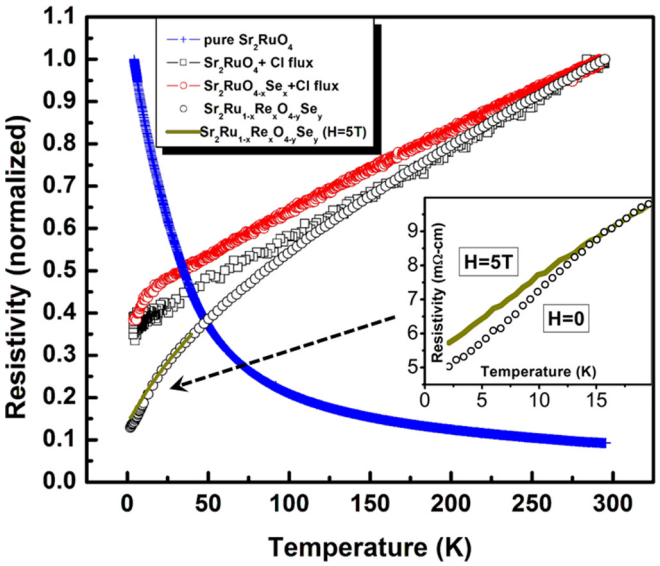

FIG. 1. Drastic change in resistivity of ceramic samples with initial stoichiometry $Sr_2Ru_{1-x}Re_xO_{4-y}Se_y$, $0 \leqslant x \leqslant 1$ and $0 \leqslant y \leqslant 1$. While pure samples ($x = 0$, $y = 0$) typically demonstrate semiconductor-type temperature dependence, the chlorine flux and vacuum treated samples demonstrate so-called strange metal behavior [12], and chalcogen addition introduces downturn. Both features are intriguing (more details can be found in [13]). The *inset* shows the magnetoresistivity of $Sr_2Ru_{1-x}Re_xO_{4-y}Se_y$.

for oxygen. Since this inclination might have been related with a superconducting phase, the efforts were focused on deepening it using, in particular, cationic substitutions for Ru. The best results were observed with Re ions [13]. At the time of publication [13], the critical temperatures in the range of 20–30 K appeared very unusual for ruthenates; however, they were later supported by the findings of Ref. [8]. Our current spectroscopic data is in support of a superconducting phase in polycrystalline $Sr_2Ru_{1-x}Re_xO_{4-y}Se_y$.

II. EXPERIMENTAL DETAILS

Details on the preparation of $Sr_2Ru_{1-x}Re_xO_{4-y}Se_y$ samples can be found in [13]. Here, we will briefly summarize them. The precursors, RuO_2, SrSe, ReO_2, $SrCO_3$, and $SrCl_2 6H_2O$, were powdered and mixed in stoichiometric proportions. A combination of hand and mechanical grinding and mixing was applied. The powder was calcined at 695 °C for 10 h, which incurred 6% of weight loss. The calcined powder was again powderized and heat treated in air, linearly increasing temperature up to 1350 °C and down during 8 h with 25% of weight loss. This powder was pelletized and heat treated again at 1350 °C in air for 5 h with linear temperature increase and decrease at a similar rate (4 h each, with a weight loss ∼5%). For optimizing heat treatment temperatures, powder thermogravimetry was used. Next, heat treatment of the pellet was performed in high vacuum ($\sim 10^{-6}$ mbar, 650 °C, 500 min). The weight of the pellet did not change noticeably, but the resistivity became smaller. No changes in the sample's characteristics were obtained at further vacuum heat treatments.

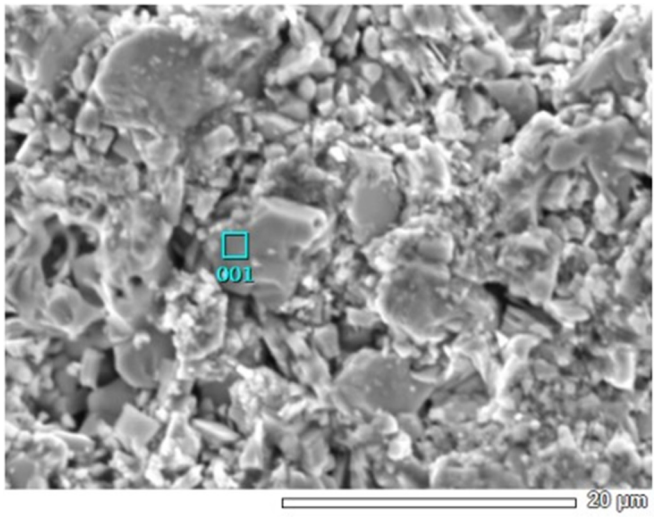

FIG. 2. Polycrystalline surface morphology of the measured sample (JEOL JCM 6000Plus SEM). The rectangle indicates one of the regions from which the compositional data were taken.

The crystalline structure of the sample is shown in Fig. 2. Using EDX well-matching data taken by multiple analysis of various crystalline areas of this sample, the composition of the sample was determined as $Sr_{2.61}(Ru_{1.20}, Re_{0.15})O_4$. In view of >25% of weight loss at the thermal treatment quoted above, the change of the initial stoichiometry is not surprising (for convenience, we will keep calling our sample $Sr_2Ru_{1-x}Re_xO_{4-y}Se_y$). For Se content, EDX microanalysis is not sufficiently sensitive. WDX analysis reveals Se of the amount less than 0.1%.

For XRD structural studies (by Rigaku Miniflex 600, measurement using Cu-K_α line in the angle interval $2\theta =$ 3–140° with the step 0.01° and scanning rate 0.1–0.5°/s; the phase content and refinement of atomic structural models was performed by the Panalytical HighScore Plus 3.0e software); 0.5 mm^3 of sample was ground in agate mortar. This analysis revealed the presence of three major phases: $Sr_3Ru_2O_7$ (50–60%), Sr_2RuO_4 (20–30%), and $SrRuO_3$ (10–20%). The lattice parameters for the phase $Sr_2(Ru, Re)(O, Se)_4$ are $a = b = 3.8745(5)$ Å and $c =$ 12.648(2) Å, with space group $I4/mmm$. For a comparison, the pure $n = 1$ phase has the parameters $a = b =$ 3.8724 Å and $c = 12.7423$ Å with the same space group [14]. This means that the lattice parameters of this cell are squeezed by 0.74% along the c axis and extended by 0.054% within the ab plane. This can be associated with a uniaxial pressure which essentially affects the T_c of Sr_2RuO_4 [15]. The lattice parameters for the phase $Sr_3(Ru, Re)_2(O, Se)_7$ are $a = b = 3.8804(2)$ Å and $c = 20.664(1)$ Å, with space group $I4/mmm$. Reference data for $n = 2$ [16] are $a = b =$ 3.8872(4) Å and $c = 20.732(3)$ Å. In this case, all the lattice parameters are squeezed (0.17% for a; 0.33% for c).

Physical characterization of properties of this sample's magnetoresistance, heat capacity, and dc and ac magnetic susceptibility were reported in [13] (sample no. 643), and we will use them later when discussing the major topic of this Rapid Communication.

For far-infrared (FTIR) measurements, a thin (about 50 micrometers) disk-type slice was dry cut from cylindrical sample no. 643 (diameter of 4 mm) using a Princeton Scientific WS25 High Precision diamond-impregnated wire saw. One face of this polycrystalline slice was carefully polished with the Precision polishing system Allied MultiPrep 8″ using diamond disk with 1 μm grade to obtain a shiny, highly planar (within 1–2° accuracy) surface. The infrared (IR) reflectivity spectra were measured at near normal incidence (≈11°) in the spectral range of 40–670 cm^{-1} (5–83 meV) at various temperatures between 5 K and 300 K using a conventional Fourier transform IR spectrometer (IFS 125HR, Bruker) equipped with a liquid He-cooled Si-bolometer and a multilayer Mylar beam splitter. For IR measurements, the polished slice was mounted with the STYCAST 2850ft epoxy glue to the tip of the nonreflective cone to avoid parasitic backreflections. A similar cone supports the gold reference mirror. Both cones were attached to the two-position sample holder on the cold finger of the vertical Konti Spectro A continuous-flow cryostat with TPX windows. The design of the cryostat provides a sliding heat exchanger with the precision positioning system controlled by stepping motors. The possible uncertainties related to misalignments during the taking of reference measurements, especially at low frequencies, can be greatly reduced in relative measurements by cycling the temperature without moving the sample [17]. The advantage of this technique is that all temperature-driven distortions of the optical setup are already frozen around 20 K, thus making it unnecessary to take a reference measurement at every temperature from 5 to 45 K. At energies below 5 meV, the small size of the sample, combined with strong oscillations that stem from standing waves in the optical elements of the spectrometer and cryostat windows, prevents accurate measurements and sets a lower limit in our experiment.

III. RESULTS

Final outcome of our FTIR spectroscopic study is shown in Fig. 3. It presents the curves that correspond to the ratios of intensity reflected by the sample at temperatures 5, 10, 15, 20, 25, and 35 K to the one at 45 K (some of them are acquired multiple times with averaging). For wave numbers $k > 220$ cm^{-1} the set of curves for different temperatures becomes nearly horizontal, indicating that at these frequencies the photon energy is noticeably above the superconducting energy gap 2Δ. In an attempt to reduce the experimental error, we minimized spreading between the curves at this high-frequency end by tiny vertical shifts towards the reflectivity ratio $= 1$. This does not affect their shapes and positions on the wave number axis important for further analysis and fitting, which required finer vertical adjustment performed curve by curve, as described in online Supplemental Material [18]. We also eliminated unimportant tails of the curves at 350 $cm^{-1} < k < 670$ cm^{-1}. At the lower wave numbers, $k \sim$ 40–225 cm^{-1}, one can observe complex structure. The most noticeable are the first dip, which occurs within the range 75–175 cm^{-1} and the peak at 50–70 cm^{-1}. The curve corresponding to the ratio R(35K)/R(45K) has the lowest deviation (i.e., it does not have as deep of a dip compared to other curves). The increase while cooling below T_c of the amplitude

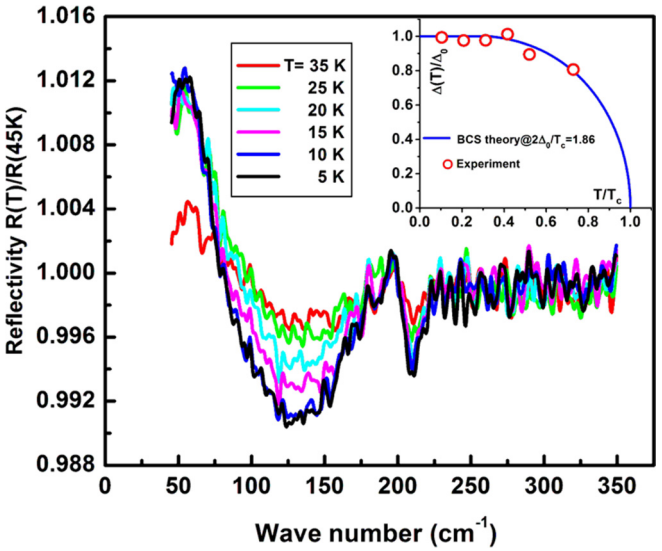

FIG. 3. Reflectivity ratios of $Sr_2Ru_{1-x}Re_xO_{4-y}Se_y$ at various temperatures and corresponding BCS fits. *Inset* illustrates correspondence of gap values with BCS theory.

of the observed structure and its disappearance at $T > 45$ K, together with a specific shape of the curves resembling that of a superconductor (see, e.g., Refs. [19,20] and Supplemental Material [18]), motivated us to analyze the possible cause of peculiarity in reflectivity at wave numbers below 200 cm^{-1} as superconductivity. A striking factor is that the curves have maximum and minimum values. Very pronouncedly, in the area of minimum, the higher the temperature, the shallower the dip. Additionally, the lower temperature curves in the area of maximum are grouped close to each other, as should be expected for the BCS model because of the plateau in $\Delta(T)$ dependence in the case $T < 0.35T_c$. Also, relative flatness of the $T = 35$ K curve means relative closeness of T to T_c. After this analysis, it becomes clear that the reflectivity of the sample in the range 0–350 cm^{-1} is determined by three components: superconducting, nonsuperconducting (in accordance with the multiphase nature of the material as described above in Sec. II), and an absorption line at around 210 cm^{-1}; see Fig. 4.

We used traditional fitting methods based on the approach suggested by Zimmermann *et al.* [21] (see Supplemental Material [18] for details) for describing the outcome of our observations. For a superconducting state the most valuable corollaries are superconducting gap values $2\Delta = 62$, 61, 61, 63, 55, and 50 cm^{-1} obtained for $T = 5$, 10, 15, 20, 25, and 35 K correspondingly. These values are plotted in *inset* to Fig. 3 on the BCS-type curve $\Delta(T)$ with $T_c \approx 48$ K. The critical temperature $T_c \approx 48$ K results in a ratio $2\Delta_0/T_c \approx 1.86$, which is somewhat lower than the BCS value 3.53 for ordinary BCS superconductors. However, in many cases this value can be different. For example, for strong coupling superconductors, including disordered YBCO superconductors, this ratio can be significantly larger [22,23]. Another example is gapless superconductivity, in which case the gap is negligibly small and T_c is finite [24]. Smaller values are also reported for finite-gap superconductors; for example, for the boron-doped diamond results [19,20] shown in the Supplemental Material

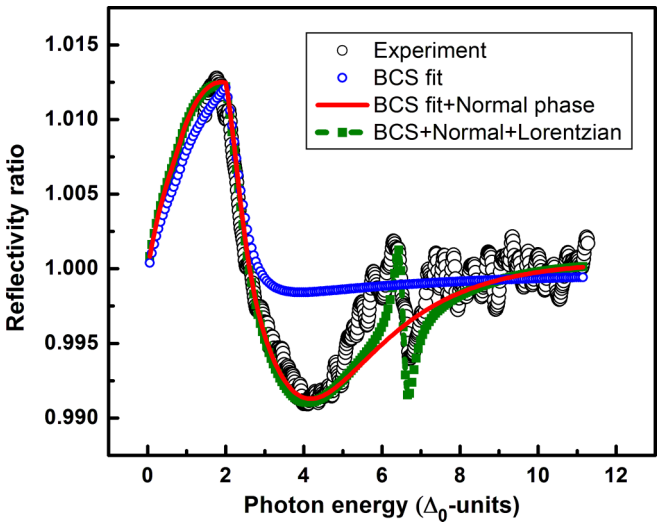

FIG. 4. Reflectivity ratio $R(T)/R(45\ \mathrm{K})$ (large circles taken at $T = 5$ K) is well fit by three model constituents: superconducting phase (BCS fit), normal phase (modified Drude fit), and an absorption line (Lorentzian fit). Fitting parameters are described in online Supplemental Material [18].

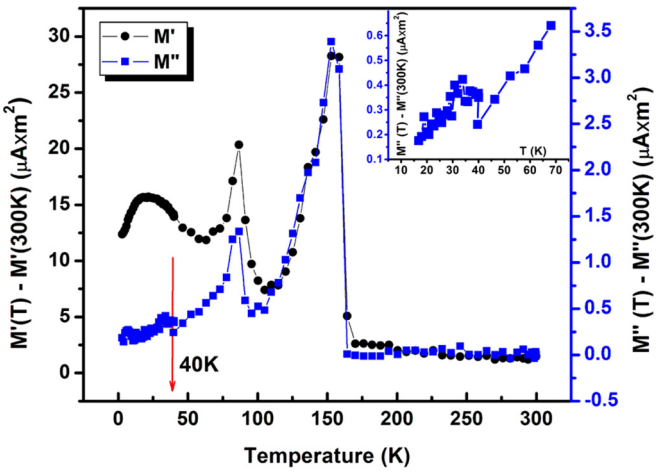

FIG. 5. ac magnetic moment $M = M' + iM''$ of $Sr_2Ru_{1-x}Re_xO_{4-y}Se_y$. Measurement with ac field of amplitude 5 Oe and frequency 337 Hz (Quantum Design PPMS). Small jump at $T > 40$ K of M'' is indicative of superconducting transition [31–35]. These curves have no hysteresis: ZFC and FC curves coincide, which means that the applied magnetic field is above H_{c1}.

[18], this ratio is 3. Large deviations of the BCS ratio towards smaller values have been considered (see, e.g., Refs. [25] and [26]). An interesting mechanism which could take place in superconductors with relatively small Fermi energies is described in [27]. In this model, $2\Delta_0/T_c$ may be arbitrarily small for small values of electron density. While it is too premature to make any quantitative comparisons between the model predictions [27] and the experimental observations, one should not ignore the fact that the plasma frequency which was an independent outcome of our fitting is of the order $\omega_{pl} \sim 10^{15}\ \mathrm{s}^{-1}$ (see the Supplemental Material [18]), which is indicative of small electron density, $n \approx 2.35 \times 10^{19}\ \mathrm{cm}^{-3}$ if $m_{\mathrm{eff}} \approx 0.1 m_e$, and thus some parallels with Ref. [27] are possible.

Aside from superconducting features, the experimental curves (Fig. 3) also contain a wide, deep dip that can be attributed to the presence of a finite amount of a normal phase. Estimates made on modified Drude-based formulas for reflectivity (see details in the Supplemental Material [18]) yield about 15 vol. % of this phase.

A second dip, though less noticeable, occurs within the range of $k \sim 200$–$225\ \mathrm{cm}^{-1}$. It has most likely a nonsuperconducting origin. Its presence was modeled via a Lorentzian absorption line (Fig. 4) caused by phonons. In copper oxide superconductors, phonon modes reveal themselves typically in the mid-IR range [28,29]; however, phonon lines have been reported in the FIR range as well [30]. One can expect the same for ruthenium oxides/chalcogenides. At the same time, as mentioned above (see also discussion below) our material has a magnetic phase which reveals magnetization below 165 K. This provides an alternative for fitting it by a magnetic Lorentzian. The latter one is shown in Fig. S4 of the online Supplemental Material [18] (together with related quantitative parameters for both Lorentzians). These Lorentzians have only a minor influence on the outcome of the superconducting fit.

IV. DISCUSSION

Let us consider how this spectroscopic result relates with other indications of possible superconductivity in this material. In addition to previously reported data [13], we performed ac susceptibility measurements; see Fig. 5. Typically, for ac magnetic susceptibility measurements, the superconducting transition reveals itself as a small jump at $T = T_c$ on the imaginary part of the magnetic susceptibility [31]. Such a jump is indeed observable on the M'' curve of our sample at about 40 K, which is supportive of superconductivity indication from the FTIR data (Fig. 3). Somewhat lower T_c in this case can be explained by the fact that the measurement was performed on an as-prepared sample, whereas, for spectroscopy, the sample was polished. After further cooling, the polycrystalline samples with intergranular connections may have a broad hump [32–35] similar to the one seen in Fig. 5. Interestingly, the major downturn of the real part of M' which may be indicative of the Meissner effect, as well as the downturn of the magnetic moment measured by the dc magnetometer [13], starts at about 20 K. The heat capacity data confirm that possible superconducting transition in the volume of the sample starts at lower temperature. These data, which were reported in [13], become much more elucidating after replotting (Fig. 6). The curve in this figure is compatible with the BCS behavior of the heat capacity of a superconductor with a broad distribution of transition temperatures, which most likely is related with superconductivity in the heterophase $Sr_2Ru_{1-x}Re_xO_{4-y}Se_y$. To characterize its behavior, as shown in Fig. 6, we applied a 5 T magnetic field to the sample, which reduced the superconductor volume mimicking its normal state value for the heat capacity. One can conclude that, at about 23 K, the heat capacity has an upturn compared to its normal value and, far below transition, it has values lower than in its normal state (as should be expected from the qualitative BCS pattern of superconductivity). Importantly, the critical temperature at this measurement is a factor of

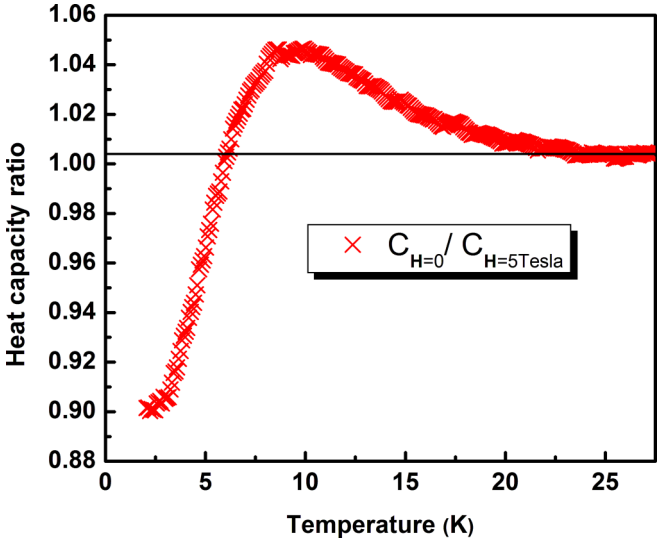

FIG. 6. Broad BCS-type singularity in temperature-dependent heat capacity of $Sr_2Ru_{1-x}Re_xO_{4-y}Se_y$, which disappears with the application of high magnetic field.

two lower than in the spectroscopic case and coincides with the essential downturn of M' in Fig. 5. A possible explanation stems from the recent results on superconductivity in calcium ruthenates [8]. Unlike 60 K superconductivity in Ca_2RuO_4 microcrystals, superconductivity in bulk polycrystalline Ca_2RuO_4 (as well as in macroscopically large crystalline) samples is fully absent [9]. If the mechanism of superconductivity in $Sr_2Ru_{1-x}Re_xO_{4-y}Se_y$ is similar to that of Ca_2RuO_4 (it is hard to expect that the mechanisms are much different), then T_c in the bulk of $Sr_2Ru_{1-x}Re_xO_{4-y}Se_y$ pellet may easily be lower than at the surface layer, even by a factor greater than 2: the heat capacity, as well as M', reflect the bulk properties while the IR reflectance, as well as M'', are related with the surface layer. We can assume that the microcrystallites in the surface layer should be relatively free from the yet unknown constraining factors imposed by the surrounding material.

Resistive transitions in our material are incomplete, most likely because of intergranular connections in which proximitized superconductivity is suppressed by the internal magnetic field, which builds up below 165 K [13] due to the presence of the $SrRuO_3$ phase in our heterophase sample. Application of a higher (5 T) external field suppresses further the resistivity downturn as the *inset* in Fig. 1 indicates.

To complete our discussion, we should point out that certain features similar to the ones which we mentioned here have been reported in the past for the composition $Sr_3Ru_2O_7$ [16]. They were attributed to magnetic fluctuations, similar to other cases [36–40]. Leaving aside the applicability of the magnetic fluctuations to all other facts pointing towards superconductivity in our samples, it is hardly possible that magnetic fluctuations would be able to quantitatively explain the spectroscopic data presented in Sec. III.

V. SUMMARY

FTIR spectroscopy, taken together with other data obtained on $Sr_2Ru_{1-x}Re_xO_{4-y}Se_y$, delivers indications of high temperature superconductivity with $T_c^{\text{onset}} > 45$ K (Fig. 3). The mentioned composition is assigned to the initial stoichiometry of samples, which after the preparation are heterophase. The crystalline structure of these phases corresponds to the Ruddlesden-Popper family strontium ruthenates with modified unit cell parameters. Most likely, the modified $n = 2$ family member stands for the possible superconductivity (as discussed in online Supplemental Material [18] section). The obtained spectroscopic value for T_c comes close to the estimate of T_c from the measurements of an imaginary part of the ac magnetic susceptibility (Fig. 5). Both properties are likely to be determined by the surface layer of our polycrystalline sample. Bulk characteristics, such as the heat capacity (Fig. 6) or the real part of the magnetic susceptibility (Fig. 5), which also point towards superconductivity, reveal themselves at lower temperatures. That means that the bulk properties are different from the properties of the surface layer, which sets up a bridge between our findings and the recently discovered superconductivity at 60 K in solitary micronanocrystals of Ca_2RuO_4. It is very likely that the mechanism of superconductivity is the same in both cases.

ACKNOWLEDGMENTS

We would like to express gratitude to the referees of this Rapid Communication; their critical remarks and very constructive suggestions essentially improved the content. A.D. acknowledges support by the Ministry of Science and Higher Education of the Russian Federation (Project No. RFMEFI62119X0035 and the State assignment of the FSRC "Crystallography and Photonics" RAS) and the Shared Research Center FSRC "Crystallography and Photonics" RAS in part of x-rays diffraction study. The work of Yu.A. and A.M. is carried out within the state assignment of the Ministry of Science and Higher Education of the Russian Federation (theme "Physics of high-temperature superconductors and novel quantum materials," Grant No. 0023-2019-0005). FTIR measurements were done using research equipment of the Shared Facilities Center at LPI. The work of the Chapman U. research team is supported by the US Office of Naval Research Grants No. N00014-16-1-2269, No. N00014-17-1-2972, No. N00014-18-1-2636, and No. N00014-19-1-2265.

[1] N. P. Armitage, Superconductivity mystery turns 25, Nature (London) **576**, 386 (2019).

[2] Y. Maeno, H. Hashimoto, K. Yoshida, S. Nishizaki, T. Fujita, J. G. Bednorz, and F. Lichtenberg, Superconductivity in a layered perovskite without copper, Nature (London) **372**, 532 (1994).

[3] A. P. Mackenzie and Y. Maeno, The superconductivity of Sr_2RuO_4 and the physics of spin-triplet pairing, Rev. Mod. Phys. **75**, 657 (2003).

[4] Y. Maeno, S. Kittaka, T. Nomura, S. Yonezawa, and K. Ishida, Evaluation of Spin-Triplet Superconductivity in Sr_2RuO_4, J. Phys. Soc. Jpn. **81**, 011009 (2012).

[5] C. Kallin, Chiral p-wave order in Sr_2RuO_4, Rep. Prog. Phys. **75**, 042501 (2012).

[6] Y. Liu and Z.-Q. Mao, Unconventional superconductivity in Sr_2RuO_4, Physica C **514**, 339 (2015).

[7] A. Pustogow, Y. Luo, A. Chronister, Y.-S. Su, D. A. Sokolov, F. Jerzembeck, A. P. Mackenzie, C. W. Hicks, N. Kikugawa, S. Raghu, E. D. Bauer, and S. E. Brown, Constraints on the superconducting order parameter in Sr_2RuO_4 from oxygen-17 nuclear magnetic resonance, Nature (London) **574**, 72 (2019).

[8] H. Nobukane, K. Yanagihara, Y. Kunisada, Y. Ogasawara, K. Isono, K. Nomura, K. Tanahashi, T. Nomura, T. Akiyama, and S. Tanda, Co-appearance of superconductivity and ferromagnetism in a Ca_2RuO_4 nanofilm crystal, Sci. Rep. **10**, 3462 (2020).

[9] M. Braden, G. André, S. Nakatsuji, and Y. Maeno, Crystal and magnetic structure of Ca_2RuO_4: Magnetoelastic coupling and the metal-insulator transition, Phys. Rev. B **58**, 847 (1998).

[10] J. Zhang, A. S. McLeod, Q. Han, X. Chen, H. A. Bechtel, Z. Yao, S. N. Gilbert Corder, T. Ciavatti, T. H. Tao, M. Aronson, G. L. Carr, M. C. Martin, C. Sow, S. Yonezawa, F. Nakamura, I. Terasaki, D. N. Basov, A. J. Millis, Y. Maeno, and M. Liu, Nano-Resolved Current-Induced Insulator-Metal Transition in the Mott Insulator Ca_2RuO_4, Phys. Rev. X **9**, 011032 (2019).

[11] Hereafter, we use terminology of the original publication [8].

[12] J. A. N. Bruin, H. Sakai, R. S. Perry, and A. P. Mackenzie, Similarity of scattering rates in metals showing T-linear resistivity, Science **339**, 804 (2013).

[13] A. M. Gulian and V. R. Nikoghosyan, Serendipitous vs. systematic search for room-temperature superconductivity, Quantum Stud.: Math. Found. **5**, 161 (2018).

[14] J. J. Neumeier, M. F. Hundley, M. G. Smith, J. D. Thompson, C. Allgeier, H. Xie, W. Yelon, and J. S. Kim, Magnetic, thermal, transport, and structural properties of $Sr_2RuO_{4+\delta}$: Enhanced charge-carrier mass in a nearly metallic oxide, Phys. Rev. B **50**, 17910 (1994).

[15] A. Steppke, L. Zhao, M. E. Barber, T. Scaffidi, F. Jerzembeck, H. Rosner, A. S. Gibbs, Y. Maeno, S. H. Simon, A. P. Mackenzie, and C. W. Hicks, Strong peak in T_c of Sr_2RuO_4 under uniaxial pressure, Science **355**, eaaf9398 (2017).

[16] S.-I. Ikeda, Y. Maeno, S. Nakatsuji, M. Kosaka, and Y. Uwatoko, Ground state in $Sr_3Ru_2O_7$: Fermi liquid close to a ferromagnetic instability, Phys. Rev. B **62**, R6089(R) (2000).

[17] A. Perucchi, L. Baldassarre, B. Joseph, S. Lupi, S. Lee, C. B. Eom, J. Jiang, J. D. Weiss, E. E. Hellstrom, and P. Dore, Transmittance and reflectance measurements at terahertz frequencies on a superconducting $BaFe_{1.84}Co_{0.16}As_2$ ultrathin film: An analysis of the optical gaps in the Co-doped $BaFe_2As_2$ pnictide, Eur. Phys. J. B **86**, 274 (2013).

[18] See Supplemental Material at http://link.aps.org/supplemental/10.1103/PhysRevResearch.2.042020 for details of fitting procedures.

[19] M. Ortolani, S. Lupi, L. Baldassarre, U. Schade, P. Calvani, Y. Takano, M. Nagao, T. Takenouchi, and H. Kawarada, Low-Energy Electrodynamics of Superconducting Diamond, Phys. Rev. Lett. **97**, 097002 (2006).

[20] S. Lupi, Terahertz spectroscopy of novel superconductors, Adv. Condens. Matter Phys. **2011**, 816906 (2011).

[21] W. Zimmermann, E. Brandt, M. Bauer, E. Seider, and L. Genzel, Optical conductivity of BCS superconductors with arbitrary purity, Physica C **183**, 99 (1991).

[22] J. F. Dodaro and S. A. Kivelson, Generalization of Anderson's theorem for disordered superconductors, Phys. Rev. B **98**, 174503 (2018).

[23] C. Pakokthom, B. Krunavakarn, P. Udomsamuthirun, and S. Yoksan, Reduced-gap ratio of high-T_c cuprates within the *d*-wave two-dimensional Van Hove scenario, J. Supercond. **11**, 429 (1998).

[24] A. A. Abrikosov and L. P. Gor'kov, Contribution to the theory of superconducting alloys with paramagnetic impurities, Zh. Eksp. Teor. Fiz. **39**, 1781 (1960) [Sov. Phys. JETP **12**, 1243 (1961)].

[25] M. Dressel, Electrodynamics of metallic superconductors, Adv. Condens. Matter Phys. **2013**, 104379 (2013).

[26] D.-V. Anghel, New phenomenology from an old theory-The BCS theory of superconductivity revisited, Physica A **531**, 121804 (2019).

[27] D. Valentinis, D. van der Marel, and C. Berthod, BCS superconductivity near the band edge: Exact results for one and several bands, Phys. Rev. B **94**, 024511 (2016).

[28] A. R. Kumar, Z. M. Zhang, V. A. Boychev, D. B. Tanner, L. R. Vale, and D. A. Rudman, Far-Infrared Transmittance and Reflectance of $YBa_2Cu_3O_{7-x}$ Films on Si Substrates, J. Heat Transfer **121**, 844 (1999).

[29] B. I. Choi, Z. M. Zhang, M. I. Flik, and T. Siegrist, Radiative Properties of Y-Ba-Cu-0 Films With Variable Oxygen Content, J. Heat Transfer **114**, 958 (1992).

[30] C. Bernhard, J. Humlícek, and B. Keimer, Far-infrared ellipsometry using a synchrotron light source-the dielectric response of the cuprate high T_c superconductors, Thin Solid Films **455–456**, 143 (2004).

[31] M. Couach, A. Khoder, and F. Monnier, Study of superconductors by a.c. susceptibility, Cryogenics **25**, 695 (1985).

[32] R. B. Goldfarb, M. Lelental, and C. A. Thompson, Alternating-field susceptometry and magnetic susceptibility of superconductors, in *Magnetic Susceptibility of Superconductors and Other Spin Systems*, edited by R. A. Hein, T. L. Francavilla, and D. H. Liebenberg (Springer US, Boston, MA, 1991), pp. 49–80.

[33] K.-H. Müller, Detailed theory of the magnetic response of high-temperature ceramic superconductors, in *Magnetic Susceptibility of Superconductors and Other Spin Systems*, edited by R. A. Hein, T. L. Francavilla, and D. H. Liebenberg (Springer US, Boston, MA, 1991), pp. 229–250.

[34] F. Gömöry, Responses of high T_c superconductors to various combinations of AC and DC magnetic fields, in *Magnetic Susceptibility of Superconductors and Other Spin Systems*, edited by R. A. Hein, T. L. Francavilla, and D. H. Liebenberg (Springer US, Boston, MA, 1991), pp. 289–311.

[35] L. Civale, T. K. Worthington, L. Krusin-Elbaum, and F. Holtzberg, Nonlinear A.C. susceptibility response near the irreversibility line, in *Magnetic Susceptibility of Superconductors and Other Spin Systems*, edited by R. A. Hein, T. L. Francavilla, and D. H. Liebenberg (Springer US, Boston, MA, 1991), pp. 313–332.

[36] T. Jarlborg and A. J. Freeman, Magnetism and superconductivity in *C*15 compounds from self-consistent band calculations, Phys. Rev. B **22**, 2332 (1980).

[37] F. M. Mueller, A. J. Freeman, J. O. Dimmock, and A. M. Furdyna, Electronic structure of palladium, Phys. Rev. B **1**, 4617 (1970).

[38] S. Nakatsuji and Y. Maeno, Quasi-Two-Dimensional Mott Transition System $Ca_{2-x}Sr_xRuO_4$, Phys. Rev. Lett. **84**, 2666 (2000).

[39] C. Pfleiderer, G. J. McMullan, S. R. Julian, and G. G. Lonzarich, Magnetic quantum phase transition in MnSi under hydrostatic pressure, Phys. Rev. B **55**, 8330 (1997).

[40] K. Yoshida, F. Nakamura, T. Goko, T. Fujita, Y. Maeno, Y. Mori, and S. NishiZaki, Electronic crossover in the highly anisotropic normal state of Sr_2RuO_4 from pressure effects on electrical resistivity, Phys. Rev. B **58**, 15062 (1998).